

SUN Xue-ming, ZHANG Hui-jian, ZUO Meng,
GU Wan-yi, XU Da-xiong

Impact of polarization mode dispersion and nonlinear effect on 40 Gbit/s dense wavelength division multiplexing system

© Higher Education Press and Springer-Verlag 2006

Abstract Dense wavelength division multiplexing (DWDM) system is the ultimate selection as an optical communication system because of its high speeds and capacities. However, the fiber nonlinear effects and polarization mode dispersion severely limit the performance of the system when signal propagates at 40 Gbit/s in a single channel. The coupled nonlinear Schrödinger equations of a single channel in DWDM, which are all considered factors of group velocity dispersion (GVD), self phase modulation (SPM), cross phase modulation (XPM), four wave mixing (FWM) and polarization mode dispersion (PMD), are derived, while their number results are obtained with extended split-step Fourier method. Finally, to analyze the impacts of the fiber nonlinear effects and PMD on the optical communication system, the simulated results of an 8×40 Gbit/s DWDM system are discussed under different conditions respectively.

Keywords optical communication system, DWDM, nonlinear effect, PMD

1 Introduction

DWDM system with channel data rates of 40 Gbit/s is the

Translated from *Acta Optica Sinica*, 2004, 24(10): 1363–1369 (in Chinese)

SUN Xue-ming(✉)
Optical Communications Center,
Beijing University of Posts and Telecommunications,
Beijing 100876, China
Department of Basic Courses,
Beijing Electronic and Science Technology Institute,
Beijing 100070, China
E-mail: sxm@besti.edu.cn

ZHANG Hui-jian, ZUO Meng, GU Wan-yi, XU Da-xiong
Beijing Electronic and Science Technology Institute,
Beijing 100070, China

tendency of optical fiber transmission systems for its advantages of higher spectrum efficiency and lower cost per bit per kilometer [1]. However, it brings us new challenges as well: The first and higher order chromatic dispersion are inferior to the signal seriously because of broader spectrum, which must be compensated [2, 3]. The narrow signal pulse suffers more from optical fiber nonlinear effects and PMD, which must be focused on especially in 40 Gbit/s DWDM system. If PMD value of optical fiber is 0.5 ps/km^{1/2} (the typical PMD value of many installed fibers), Gaussian pulse can transmit only 25 km in it at 1 dB power penalty. Simultaneously, the combination of PMD and nonlinear effects results in more complexity. Therefore all factors, which influence the signal, must be considered in designing the optical communication system. In this paper, the coupled nonlinear Schrödinger equations of a single channel in DWDM are derived, which takes all factors of GVD, SPM, XPM, FWM and PMD into consideration, with the numerical results shown.

2 Theory analysis

The mathematical model of concatenated polarization maintained fiber (PMF) can represent the activity of PMD in actual fiber as shown in Fig. 1, where l_0 is the length of each PMF; $\Delta\tau_i$, which equals to $\Delta\tau_0$ in this paper, is the delay difference between the fast axis and slow axis of PMF i . θ_i is the angle formed by the fast axis of PMF i and the X axis of the fixed coordinate system; $(\theta_{i+1} - \theta_i)$, random variables independent of each other, are uniformly distributed and range from 0 to 2π . The PMD coefficient expression of the model is shown below:

$$D_{\text{PMD}} = \sqrt{\frac{8}{3\pi l_0}} \Delta\tau_0 = \sqrt{\frac{8}{3\pi}} \frac{\Delta n}{c} \sqrt{l_0} \quad (1)$$

where Δn is the refractive index difference between the fast axis and slow axis, and c is the velocity of light in vacuum. When the value of the PMD coefficient is given, Δn

can be evaluated according to Eq. (1).

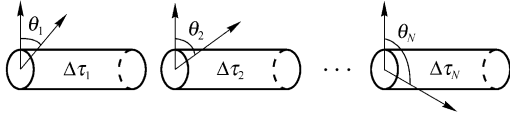


Fig. 1 Sketch map of polarization maintained fiber concatenation model

The transmission of the optical signal along the optical fiber satisfies nonlinear Schrödinger equations. Now we begin to derive the equations that depict the optical signal transmission along PMF in a DWDM system with N channels. In the optical communication area, the envelope of optical signal is of specific interest. Suppose the electric field of channel l can be described as:

$$\begin{aligned} \mathbf{E}_l(\mathbf{r}, t) &= \frac{1}{2} \begin{pmatrix} F_l(x, y) A_{lx}(z, t) \exp[i(\omega_l t - \beta_{lx} z)] + c.c. \\ F_l(x, y) A_{ly}(z, t) \exp[i(\omega_l t - \beta_{ly} z)] + c.c. \\ 0 \end{pmatrix} \\ &= \frac{1}{2} \begin{pmatrix} F(x, y) A_{lx}(z, t) \exp[i(\omega_l t - \beta_{lx} z)] + c.c. \\ F(x, y) A_{ly}(z, t) \exp[i(\omega_l t - \beta_{ly} z)] + c.c. \\ 0 \end{pmatrix} \end{aligned} \quad (2)$$

where $F_l(x, y)$ is the transverse mode of channel l , which equals to $F(x, y)$ approximately in the case of single mode transmission. $A_{lp}(z, t)$ and β_{lp} are the slowly varying envelope and transmission constant of $p(p = x, y)$ component of channel l , respectively. The composite electric field of N channels can be written as:

$$\begin{aligned} \mathbf{E}(\mathbf{r}, t) &= \frac{1}{2} \begin{pmatrix} \sum_{l=1}^N F(x, y) A_{lx}(z, t) \exp[i(\omega_l t - \beta_{lx} z)] + c.c. \\ \sum_{l=1}^N F(x, y) A_{ly}(z, t) \exp[i(\omega_l t - \beta_{ly} z)] + c.c. \\ 0 \end{pmatrix} \\ &= \frac{1}{2} \begin{pmatrix} \sum_{l=1}^N E_{lx} \exp[i(\omega_l t - \beta_{lx} z)] + c.c. \\ \sum_{l=1}^N E_{ly} \exp[i(\omega_l t - \beta_{ly} z)] + c.c. \\ 0 \end{pmatrix} \end{aligned} \quad (3)$$

here $E_{lp} = F(x, y) A_{lp}(z, t)$

Nonlinear electric susceptibility can be written as:

$$\mathbf{P}_{NL}(\mathbf{r}, t) = \varepsilon_0 \chi^{(3)} \vdots \mathbf{E} \mathbf{E} \mathbf{E} = \varepsilon_0 \begin{pmatrix} \sum_{rst} \chi_{xrst}^{(3)} E_r E_s E_t \\ \sum_{rst} \chi_{yrst}^{(3)} E_r E_s E_t \\ 0 \end{pmatrix} \quad (4)$$

where $r, s, t = x, y, z$, x and y are the intrinsic axes of PMF. The following equation is for quartz fiber:

$$\chi_{xyxy}^{(3)} = \chi_{xyxy}^{(3)} = \chi_{xyyx}^{(3)} = \frac{1}{3} \chi_{xxxx}^{(3)}$$

In addition, $\mathbf{P}_{NL}(\mathbf{r}, t)$ can also be written as:

$$\mathbf{P}_{NL}(\mathbf{r}, t) = \frac{1}{2} \begin{pmatrix} \sum_{l=1}^N P_{lx} \exp[i(\omega_l t - \beta_{lx} z)] + c.c. \\ \sum_{l=1}^N P_{ly} \exp[i(\omega_l t - \beta_{ly} z)] + c.c. \\ 0 \end{pmatrix} \quad (5)$$

Substituting Eq. (3) into Eq. (4) and comparing Eq. (4) with Eq. (5), we have

$$\begin{aligned} P_{lx} &= \frac{3\varepsilon_0 \chi_{xxxx}^{(3)}}{4} \{ |E_{lx}|^2 + 2 \sum_{j=1, j \neq l}^N |E_{jx}|^2 + \frac{2}{3} \sum_{j=1}^N |E_{jy}|^2 \} E_{lx} \\ &+ \sum_{\substack{j, k, m, j \neq m, k \neq m \\ \omega_j = \omega_j + \omega_k - \omega_m}} (2 - \delta_{jk}) E_{jx} E_{kx} E_{mx}^* \exp[i(\beta_{lx} + \beta_{mx} - \beta_{jx} - \beta_{kx})z] \\ &+ \frac{2}{3} \sum_{\substack{j, k, m, k \neq m \\ \omega_j = \omega_j + \omega_k - \omega_m}} E_{jx} E_{ky} E_{my}^* \exp[i(\beta_{lx} + \beta_{my} - \beta_{jx} - \beta_{ky})z] \\ &+ \frac{1}{3} \sum_{\substack{j, k, m \\ \omega_j = \omega_j + \omega_k - \omega_m}} (2 - \delta_{jk}) E_{jy} E_{ky} E_{mx}^* \exp[i(\beta_{lx} + \beta_{mx} - \beta_{jy} - \beta_{ky})z] \end{aligned} \quad (6)$$

The first part in the brace on the right-hand side of Eq. (6) denotes SPM and XPM, while the following three parts denote FWM. FWM in fiber is mostly part degeneracy, i.e., $j = k$. Then:

$$\beta_{lx} + \beta_{mx} - \beta_{jx} - \beta_{kx} = \beta_{lx} + \beta_{mx} - 2\beta_{jx} = \beta_{jx}'' (\omega_m - \omega_j)^2$$

$$\beta_{lx} + \beta_{my} - \beta_{jx} - \beta_{ky} = \beta_{jx}'' (\omega_m - \omega_j)^2 + \frac{\Delta n}{c} (\omega_m - \omega_j)$$

$$\beta_{lx} + \beta_{mx} - \beta_{jy} - \beta_{ky} = \beta_{jx}'' (\omega_m - \omega_j)^2 - 2 \frac{\omega_j \Delta n}{c}$$

Substituting constants into equations above, we find:

$$|\beta_{jx}'' (\omega_m - \omega_j)^2| \ll \left| \beta_{jx}'' (\omega_m - \omega_j)^2 - 2 \frac{\omega_j \Delta n}{c} \right|$$

$$\left| \beta_{jx}'' (\omega_m - \omega_j)^2 + \frac{\Delta n}{c} (\omega_m - \omega_j) \right| \ll \left| \beta_{jx}'' (\omega_m - \omega_j)^2 - 2 \frac{\omega_j \Delta n}{c} \right|$$

The items on the right of the above inequation are about three orders of magnitude larger than the ones on the left. Items containing $\exp\{i[\beta_{jx}'' (\omega_m - \omega_j)^2 - 2\omega_j \Delta n/c]z\}$ can be ignored for their severe phase mismatch. Therefore, Eq. (6) can be simplified as:

$$\begin{aligned} P_{lx} &= \frac{3\varepsilon_0 \chi_{xxxx}^{(3)}}{4} \{ |E_{lx}|^2 + 2 \sum_{j=1, j \neq l}^N |E_{jx}|^2 + \frac{2}{3} \sum_{j=1}^N |E_{jy}|^2 \} E_{lx} \\ &+ \sum_{\substack{j, m, j \neq m \\ \omega_l = 2\omega_j - \omega_m}} E_{jx}^2 E_{mx}^* \exp[i\beta_{jx}'' (\omega_m - \omega_j)^2 z] \\ &+ \frac{2}{3} \sum_{\substack{j, m, j \neq m \\ \omega_l = 2\omega_j - \omega_m}} E_{jx} E_{jy} E_{my}^* \exp\{i[\beta_{jx}'' (\omega_m - \omega_j)^2 \\ &+ \frac{\Delta n}{c} (\omega_m - \omega_j)]z\} \end{aligned} \quad (7)$$

According to the derivation of nonlinear Schrödinger [4], optical fiber transmission equations suitable for DWDM

system can be obtained, which include PMD and various nonlinear effects.

$$\begin{aligned} & \frac{\partial A_{lp}}{\partial z} + \frac{\alpha}{2} A_{lp} - \beta'_{lp} \frac{\partial A_{lp}}{\partial t} + \frac{i}{2} \beta''_{lp} \frac{\partial^2 A_{lp}}{\partial t^2} + \frac{1}{6} \beta'''_{lp} \frac{\partial^3 A_{lp}}{\partial t^3} \\ &= i\gamma_l (|A_{lp}|^2 + 2 \sum_{j=1, j \neq l}^N |A_{jp}|^2 + \frac{2}{3} \sum_{j=1}^N |A_{jq}|^2) A_{lp} \\ &+ i\gamma_l \sum_{\substack{j,m,j \neq m \\ \omega_j = 2\omega_j - \omega_m}} A_{jp}^2 A_{mp}^* \exp[i\beta''_{jp} (\omega_m - \omega_j)^2 z] \\ &+ i\gamma_l \frac{2}{3} \sum_{\substack{j,m,j \neq m \\ \omega_j = 2\omega_j - \omega_m}} A_{jp} A_{jq} A_{mq}^* \exp\{i[\beta''_{jp} (\omega_m - \omega_j)^2 \\ &+ \frac{\Delta n}{c} (\omega_m - \omega_j)]z\} \end{aligned} \quad (8)$$

where $p, q = x, y$ and $p \neq q$, γ_l is the nonlinear coefficient for channel l with the definition :

$$\gamma_l = \frac{n_2 \omega_l}{c A_{\text{eff}}}$$

A_{eff} is the effective area of the fiber core. In the model shown in Fig. 1, the output signal of a PMF and the input signal of the following PMF satisfy the equation below [4, 5]:

$$\begin{pmatrix} A_{lx}^{(j+1-\text{in})} \\ A_{ly}^{(j+1-\text{in})} \end{pmatrix} = \begin{pmatrix} \cos \Psi_j & \exp(i\varphi_j) \sin \Psi_j \\ -\exp(-i\varphi_j) \sin \Psi_j & \cos \Psi_j \end{pmatrix} \begin{pmatrix} A_{lx}^{(j-\text{out})} \\ A_{ly}^{(j-\text{out})} \end{pmatrix}$$

where $(j-\text{in})$ and $(j-\text{out})$ denote the input signal and output signal of the PMF j , respectively. $\Psi_j = (\theta_{j+1} - \theta_j)$ and φ_j are random variables independent of each other with uniform probability distribution ranging from 0 to 2π .

3 Numerical simulation and analysis

Generally, Eq. (8) cannot be solved analytically but numerically. They are introduced to simulate the 8×40 Gbit/s DWDM system whose signal frequency spacing is 100 GHz. In this system, each signal is a random sequence with a hyper-Gaussian pulse of 26 bits and sample rate per code is 64. The mean power of the signal is 1 mW. Ideal EDFAs are used to compensate the loss of fiber completely. Because the input signal is a hyper-Gaussian pulse and the signal can couple in concatenation fibers, the limitation of the signal transmission distance can be ignored. Each signal channel

of the system is designed with 6 spans of G.655 fiber, 80 km in length each. Its setup is shown in Fig. 2. During the computation, step-split Fourier method is used [6]. To increase the precision, twice-iteration is adopted in each step. Random number generators in computations use the same random number seed to eliminate the impact of their randomness.

The dispersion compensation fiber (DCF) with length of 16 km and taking no account of PMD, can fully compensate the dispersion of the first channel at 1 550 nm in the transmission fiber. The typical attributes of the two kinds of fibers are shown in Table 1.

We compare the waveform and eye diagram of the input signals (Fig. 3) with those of output signals to investigate the impact of the combination of PMD and nonlinear effects on 40 Gbit/s system. There are four cases: Fig. 4(a) shows the waveform and eye diagram of the output signal in single channel system without PMD; Fig. 4(b) those in single channel system with PMD; Fig. 5(a) the waveform and eye diagram of the output of channel 1 in the 8×40 Gbit/s DWDM system without PMD; and Fig. 5(b) those of the output of channel 1 in the 8×40 Gbit/s DWDM system with PMD.

From Figs. 3–5, the conclusion can be drawn that if PMD is not taken into consideration, signal in the single channel system suffers from SPM, which results in the fluctuation of the top of the pulses. In addition, XPM and FWM in multi-wavelength systems make the signal waveform worse and the eyelid thicker. If we take PMD into consideration, the pulse becomes broader and its phase shifts randomly, which, however, restrains the impact of nonlinear effects to some extent. This is also illustrated in Fig. 6. The figure shows the eye opening penalty versus propagation distance in DWDM systems with different counts of channels. In Fig. 6, the dashed line denotes the simulation result without PMD, and the solid line, which is the average of 20 computation results for the randomness of PMD, denotes the result with PMD. When the average power of a single channel is as small as 0.1 mW, the eye-opening penalty of the system with PMD is inferior to that of the system without PMD. It shows that the impact of fiber nonlinear effects is weaker than PMD (Fig. 6(a)). If the average power of a single channel is increased to 1 mW, the eye opening penalty becomes larger than that of the 0.1 mW system (Fig. 6(b)), which shows that nonlinear effects become the major influencing factor. Furthermore, when the average power of a single channel rises to 1 mW, the eye opening penalty with PMD is better than that without PMD after transmission in

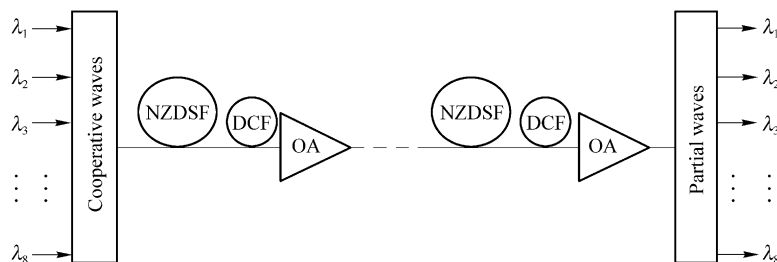


Fig. 2 Block diagram of system

Table 1 The typical attributes of two kinds of fibers

Fiber categories	G.655	DCF
Attenuation coefficient/(dB·km ⁻¹)	0.22	0.5
Effective area /μm ²	64	20
Nonlinear refractive index/(m ² ·W ⁻¹)	2.6×10 ⁻²⁰	2.6×10 ⁻²⁰
1 550 nm dispersion coefficient /(ps·km·nm ⁻¹)	3	-48
1 550 nm dispersion slop /(ps·km·nm ⁻²)	0.045	-0.7
PMD coefficient /(ps·km ^{-1/2})	0.5	—

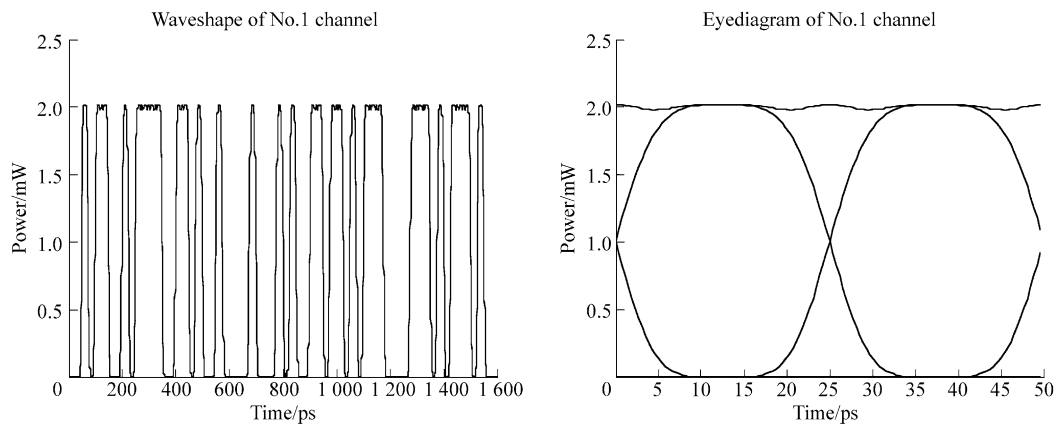


Fig. 3 Wave plot and eye diagram of original signal

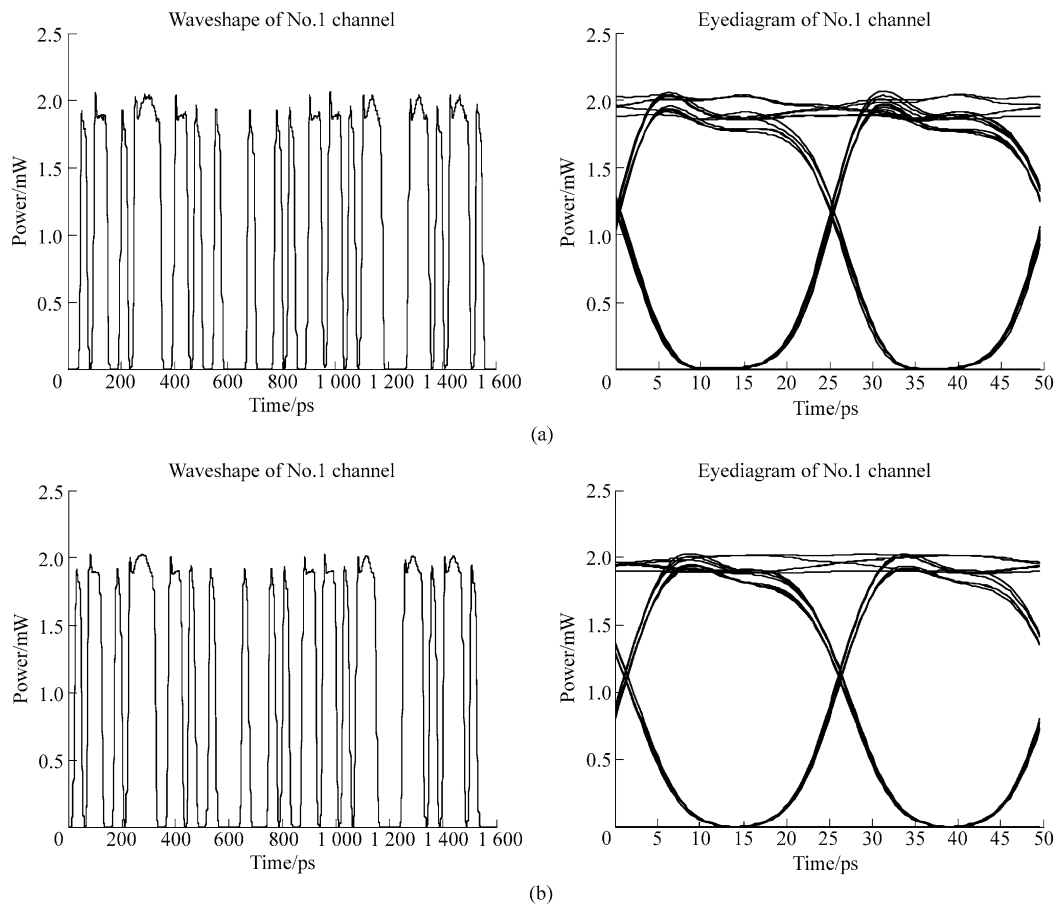


Fig. 4 Wave plot and eye diagram of single channel after propagation 480 km. (a) Without polarization mode dispersion; (b) With polarization mode dispersion

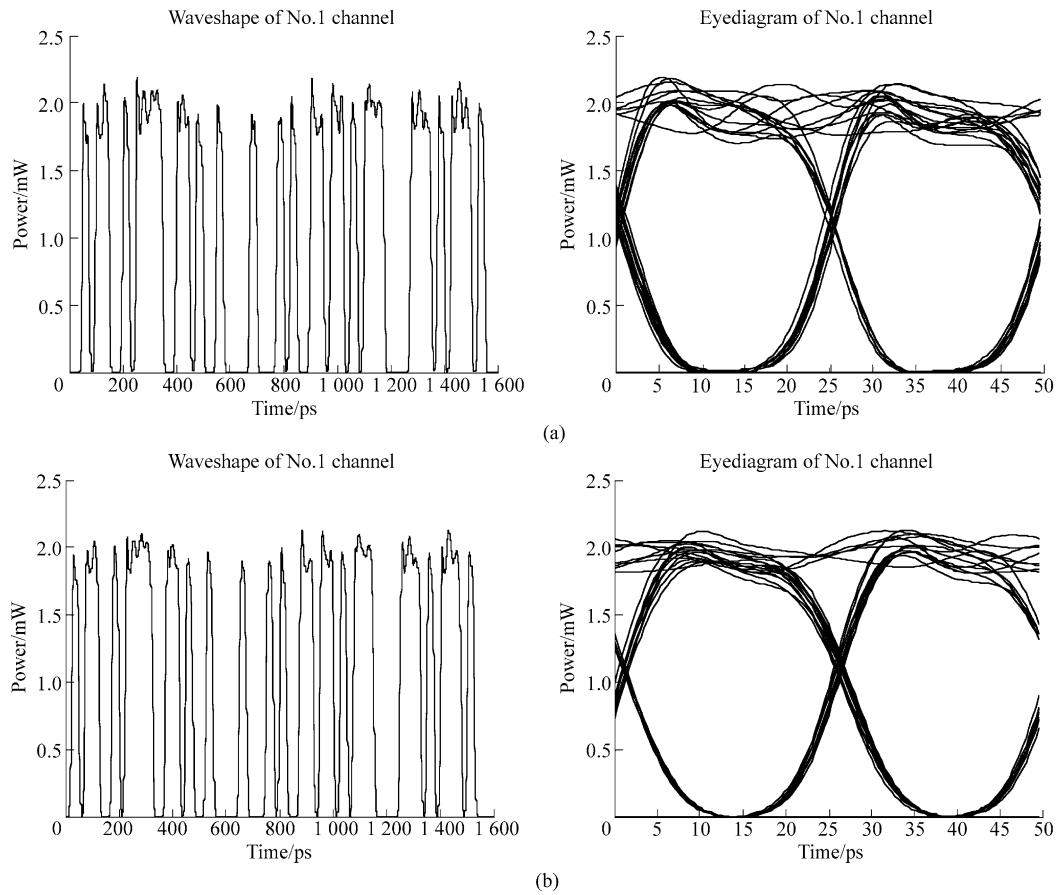


Fig. 5 Wave plot and eye diagram of No.1 of eight channels after propagation 480 km. (a) Without polarization mode dispersion; (b) With polarization mode dispersion

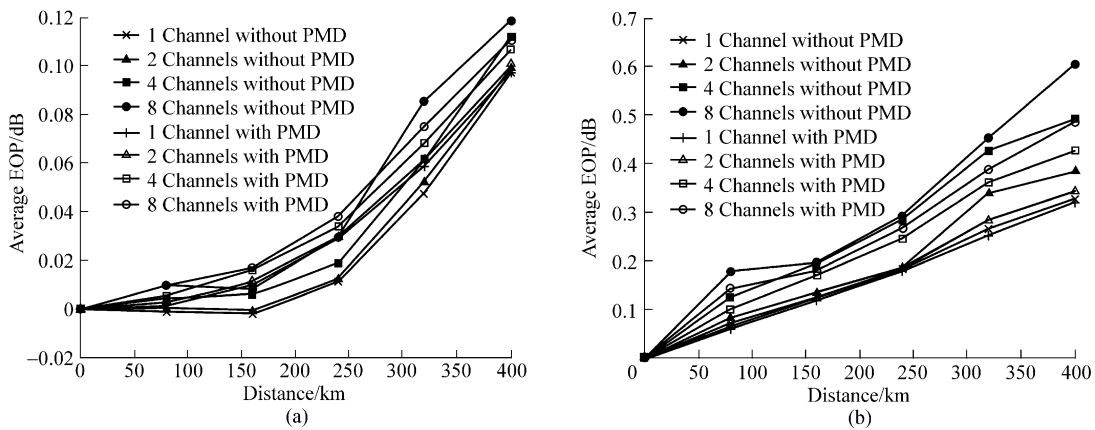


Fig. 6 Relation diagram of eye opening penalty and propagation distance. (a) The average power of a single channel is 0.1 mW; (b) The average power of a single channel is 1 mW

multi-wavelength systems. Thus far, conclusions can be drawn that, firstly, the impact of nonlinear effects is dominant for system performance, secondly, mild PMD may mitigate the impact of nonlinear effects to some degree because it can broaden the signal pulse and lower the instantaneous power of signal peak. The combination of PMD and nonlinear effects is a key

problem to conquer in a DWDM system with channel data rates of 40 Gbit/s.

4 Summary

In this paper, transmission equations of a DWDM system

including PMD, SPM, XPM and FWM are derived. Based on the equations, numerical simulations of an 8×40 Gbit/s DWDM system have been carried out. The results show that when the signal power is low, PMD has more effect on system compared with nonlinear effects. When signal power gets larger, nonlinear effects become dominating, which may be mitigated to some degree by mild PMD if we consider the effect of PMD as that of a small chromatic dispersion. The simulated results above are similar to those of the real DWDM systems. All kinds of factors should be taken into account based on the analysis above in the system. The equations and methods in this paper are valid for the design and analysis of long haul DWDM systems with high bit rates.

Acknowledgements This research was supported by the National Natural Science Foundation of China (No. 60132020) and the Hi-Tech Research and Development Program of China.

References

1. Zhu B, Nelson L., Leng L., et al., Transmission of 1.6 Tb/s (40×42.7 Gb/s) over transoceanic distance with terrestrial 100 km amplifier spans, OFC2003, FN2: 742–743
2. Ning T. G., Jian S. S. et al., 4×10 Gb/s 412 km DWDM dispersion compensation using multiwavelength chirped fiber bragg grating, ACTA OPTICA SINICA, 2002, 22(7): 839–841 (in Chinese)
3. Li T. J., Ning T. G. et al., Dispersion compensators based on overlapped linearly chirped fiber gratings for DWDM systems, Chinese Journal of Lasers, 2001, 10(6): 417–421
4. Govind P. Agrawal, Nonlinear fiber optics second edition, New York: The Institute of Optics University of Rochester, 1995
5. P. K. A. Wai, C. R. Menyuk, H. H. Chen, Stability of solitons in Randomly varying birefringent fibers, Optics letters, 1991, 16(16): 1231–1233
6. Wang J. Q., Gu W. Y., The analysis of fiber nonlinear effects, Journal of Beijing University of Posts and Telecommunications, 2003, 26(1): 73–77 (in Chinese)